Chemically Precise Glycoengineering Improves Human Insulin

Xiaoyang Guan,[†,∥] Patrick K. Chaffey,[†,∥] Xiuli Wei,[‡,∥] Daniel R Gulbranson,[§,∥] Yuan Ruan,[†] Xinfeng Wang,[†] Yaohao Li,[†] Yan Ouyang,[§] Liqun Chen,[†] Chen Zeng,[†] Theo N. Koelsch,[†] Amy H. Tran,[†] Wei Liang,*[,‡] Jingshi Shen,*[,§] and Zhongping Tan*[,†]
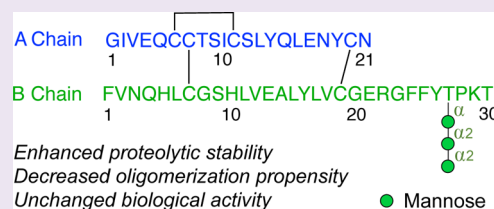
†Department of Chemistry and Biochemistry and BioFrontiers Institute, University of Colorado, Boulder, Colorado 80303, United States

‡Protein and Peptide Pharmaceutical Laboratory, Institute of Biophysics Chinese Academy of Sciences, 15 Datun Road, Beijing 100101, People's Republic of China

§Department of Molecular, Cellular, and Developmental Biology, University of Colorado, Boulder, Colorado 80303, United States

Ⓢ Supporting Information

ABSTRACT: Diabetes is a leading cause of death worldwide and results in over 3 million annual deaths. While insulin manages the disease well, many patients fail to comply with injection schedules, and despite significant investment, a more convenient oral formulation of insulin is still unavailable. Studies suggest that glycosylation may stabilize peptides for oral delivery, but the demanding production of homogeneously glycosylated peptides has hampered transition into the clinic. We report here the first total synthesis of homogeneously glycosylated insulin. After characterizing a series of insulin glycoforms with systematically varied O-glycosylation sites and structures, we demonstrate that O-mannosylation of insulin B-chain Thr27 reduces the peptide's susceptibility to proteases and self-association, both critical properties for oral dosing, while maintaining full activity. This work illustrates the promise of glycosylation as a general mechanism for regulating peptide activity and expanding its therapeutic use.

A Chain GIVEQCCTSICSLYQLENYCN
1   10   21
B Chain FVNQHLCGSHLVEALYLVCGERGFFYTPKT
1   10   20   α 30
                                    α2
                                    α2
Enhanced proteolytic stability
Decreased oligomerization propensity
Unchanged biological activity   ● Mannose

Diabetes affects more than 400 million people, and with more than 3.5 million diabetes-associated deaths annually, it is a leading cause of death worldwide.[1] Since its first clinical administration in 1922, insulin therapy has become a life-saving necessity for patients with type 1 diabetes, and a critical option for managing type 2 diabetes when other therapies fail.[2,3] Starting insulin use early in patients with type 2 diabetes leads to better glycemic control and improved long-term outcomes.[4] Although it is effective and beneficial in controlling diabetes, more than half of patients for whom insulin is recommended do not achieve its required schedule, which adversely impacts treatment outcomes.[5,6] One major reason for such low patient compliance is that, in order to achieve optimal glucose control, four or five daily injections (one or two daily injections of slow-acting insulin plus one injection of rapid-acting insulin before each meal) can be necessary, or use of an insulin pump that administers insulin through a catheter site. Frequent injections and catheters cause discomfort and inconvenience to patients and thus contribute to low compliance.[7] This issue has led many to focus research on more convenient ways of administering the drug.[8,9]

Among the new ways that have been explored, oral administration is seen as the most convenient, and perhaps ideal, route.[10] Orally absorbed insulin offers not only comfort, but it also lessens concern over side effects by more closely mimicking the physiologically natural route of insulin secretion and absorption.[11] When secreted from the pancreas, insulin is first passed to the liver via the portal vein before reaching systemic circulation. When taken orally, insulin is also absorbed into the portal vein from the small intestine (Figure 1). In
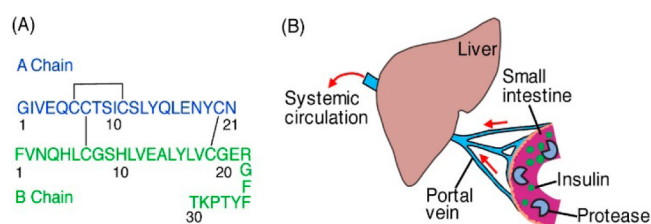

Figure 1. (A) Human insulin protein sequence and (B) a schematic illustration of the absorption pathway of insulin following its oral administration. If not degraded by intestinal proteases, insulin is absorbed into the portal vein, which transits the liver before passing the insulin into systemic circulation. This more closely mimics the route of pancreas-secreted insulin than subcutaneous injection.

contrast, insulin injected subcutaneously is released systemically and is absorbed mostly by muscle tissue. Because the liver is much more sensitive to insulin than muscle tissue, the oral route should lead to more effective glucose control compared to injected insulin, which in turn will minimize the risks

associated with the traditional insulin therapy like hypoglycemia, weight gain, and hyperinsulinemia.[11]

To date, although many synthetic insulin analogs have been explored, no orally available insulin has been approved.[12] A key challenge is the great difficulty of protecting the small peptide (Figure 1A) from the harsh conditions in the human gastrointestinal tract. If insulin is to be absorbed in the small intestine, it must survive the stomach and conditions in the small intestine.[13] Fortunately, a number of pH sensitive materials have been recently developed that are capable of protecting insulin from the environment of the stomach and selectively releasing insulin when encountering the neutral pH conditions of the small intestine.[14] Currently, this leaves insulin's low absorption in the small intestine (Figure 1B) as the major barrier standing in the way of developing oral insulin.[15,16] While several factors contribute to this problem, the main two are the vulnerability of insulin to the proteases in the small intestine and the relatively large size of oligomerized insulin.[13] Therefore, in order to realize an orally available insulin therapy, it is necessary to engineer insulin analogs that are more resistant to both proteolytic degradation and self-association.[13,17] More stable analogs will survive longer, which increases overall absorption efficiency, while individual monomers have better permeability across the intestinal epithelium compared to the larger oligomers.[18,19]

Studies with heterogeneous glycoproteins suggest that glycosylation often decreases a protein's propensity for aggregation or oligomerization and can block the action of proteases.[20,21] With insulin specifically, chemical glycosylation via non-native linker chemistries has already been shown to improve the stability of the peptide; however increased immunogenicity was reported in more heavily glycosylated analogs.[22] Fortunately, natural glycosylation linkage chemistry has been shown to decrease immunogenicity.[23,24] PEG conjugates of insulin have also shown some promise in improving its properties.[25] However, PEG polymers may significantly increase the size of the molecule and can thus lead to difficulties in peptide absorption.[26] Therefore, we chose to use glycoengineering as a way to address the natural limitations of insulin. Previous results suggest that attaching glycans to unstructured regions has the greatest chance of imparting beneficial effects, while minimizing interference with protein folding.[27−31] Studies also indicate that, while glycans can be quite large, it is predominantly the carbohydrate residues closest to the peptide backbone, the core structures, that mediate most of the physical changes.[32,33] However, these observations were made with peptides and proteins that naturally carry some amount of glycosylation, and it was unclear if these conclusions could be applied to artificially glycosylated systems, like insulin.

To take steps toward a clinically viable glycosylated insulin, we developed the first robust methods for the preparation of homogeneous glycosylated insulin. We then undertook a study to systematically compare the properties of homogeneous insulin glyco-variants, in order to identify the glycosylation sites and glycan types that confer the greatest oral bioavailability on insulin.

RESULTS AND DISCUSSION

Design and Chemical Synthesis of Homogeneous Insulin Glycoforms. We started by designing and synthesizing five different insulin glycoforms, **2−6**, each containing an α-linked N-acetylgalactosamine (GalNAcα), at either the SerA9,

SerA12, SerB9, ThrB27, or ThrB30 sites, which are located in unstructured regions across both the A and B chains of human insulin (Figure 2). ThrA8 was not used in this study because it
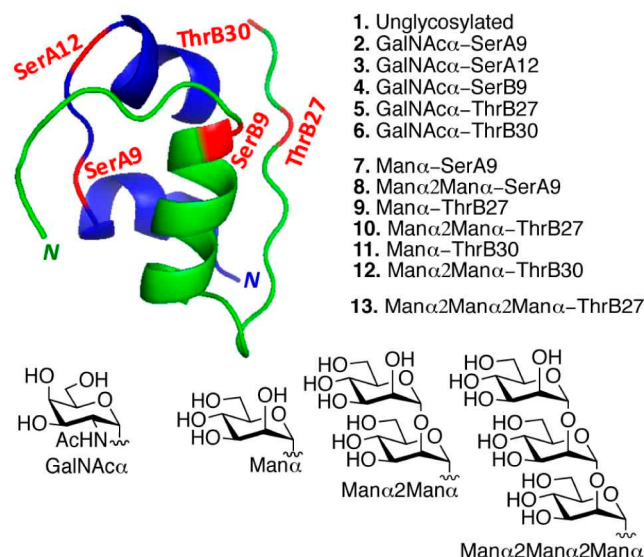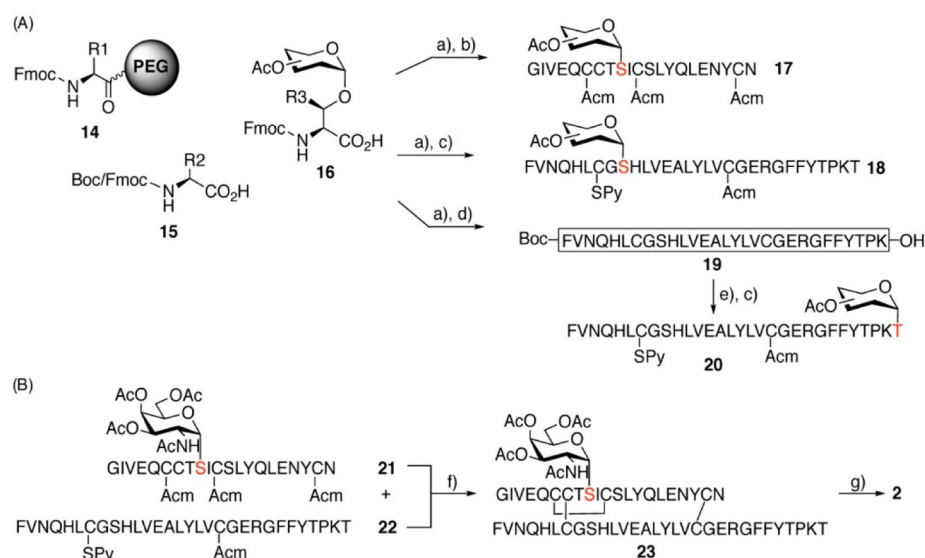

1. Unglycosylated
2. GalNAcα−SerA9
3. GalNAcα−SerA12
4. GalNAcα−SerB9
5. GalNAcα−ThrB27
6. GalNAcα−ThrB30

7. Manα−SerA9
8. Manα2Manα−SerA9
9. Manα−ThrB27
10. Manα2Manα−ThrB27
11. Manα−ThrB30
12. Manα2Manα−ThrB30

13. Manα2Manα2Manα−ThrB27

Figure 2. Structure of human insulin and glyco-variants studied in this work. The O-glycosylated Ser and Thr residues are highlighted in red. The structural feature of each glycoform is implied by its name, i.e., GalNAcα-SerA9 representing the glycoform containing a single GalNAc α-linked to the A chain Ser9 and Manα2Manα2Manα-ThrB27 representing the glycoform containing an α1,2-linked trimannose at the B chain Thr27 site.

is adjacent to SerA9 and the effects of its glycosylation can be roughly represented by those of SerA9. Together with the unglycosylated insulin **1**, this gave us a small collection of isoforms with varied glycosylation sites to study.

Unglycosylated insulin is commonly obtained via recombinant protein expression[34,35] in part because its chemical synthesis is unusually challenging.[36−39] Further complicating matters, to our knowledge, the total synthesis of glycosylated insulin has not been reported.[12] That said, total chemical synthesis of glycoproteins has made significant strides in the past decade, and over 20 glycoproteins have been made chemically.[40−48] Compared to recombinant expression methods, chemical synthesis is a more predictable, flexible, and precise way to generate molecules with small variations in glycan structure.[33,49] Therefore, we chose to use our capacity for chemical synthesis to prepare the insulin glycoforms described above.

Even with recent advances, total chemical synthesis of glycosylated insulin is challenging on two levels, the first being the glycoprotein synthesis itself and the second being accurate construction of the disulfide-linked two-chain structure of insulin.[36,37,50,51] In order to expedite our study, we first systematically optimized the reagents, procedures, and conditions to obtain simple and effective routes for the synthesis of all the glycosylated insulin analogs in this study.[30,52] As shown in Scheme 1A, the glycosylated and unglycosylated insulin chains were prepared at 0.2 g scale through the use of preloaded NovaSyn TGT resins (EMD Millipore), and HATU as the coupling agent. The glycosylated amino acid building blocks, which have relatively large side chains, were efficiently incorporated into the peptide during solid-phase peptide synthesis (SPPS) by prolonging their

Scheme 1. Synthesis of Insulin Variants[a]

[a](A) Synthesis of glycosylated insulin chains. Reagents and conditions: (a) 1. HATU, DIEA, DMF. 2. Piperidine, DBU, DMF. (b) TFA/TIS/H$_2$O (95:2.5:2.5). (c) TFA/TIS/H$_2$O (95:2.5:2.5) + 20 equiv DTDP. (d) DCM/TFE/AcOH (8:1:1). (e) H-Thr(Ac-protected sugar)–OH, EDCI, HOOBt, CHCl$_3$/TFE. **19**, side-chain fully protected peptide. R1, protected side-chains of Asn, Thr, and Lys. R2, protected side-chains of amino acids. R3, H or Me. (B) Synthesis illustrated by the preparation of the insulin glyco-variant **2**. Reagents and conditions: (f) 1. 8.0 M Gn·HCl, 0.1 M Tris·HCl, pH 8.0. 2. I$_2$, MeOH. 3. HPLC purification. (g) 1. NH$_2$–NH$_2$ (5%) in H$_2$O. 2. HPLC purification, 6.5% overall yield based on A-chain resin loading. Abbreviations: Acm, acetamidomethyl; Py, 2-pyridine; TIS, triisopropylsilane; DTDP, 2,2′-dithiodipyridine; EDCI, N′-(3-dimethylaminopropyl)-N-ethylcarbodiimide; TFE, 2,2,2-trifluoroethanol; HOOBt: hydroxy-3,4-dihydro-4-oxo-1,2,3-benzotriazine.

coupling time. Depending on the glycosylation site, the B chain was prepared either by step-by-step synthesis (e.g., **18**) or by fragment condensation in solution,[53,54] followed by the removal of the side chain protecting groups and in situ cysteine activation in a TFA/TIS/H$_2$O/DTDP cocktail (e.g., **20**; described in the Supporting Information).[52] The regioselective construction of three disulfide bonds was achieved via the formation of the intermediate dimer in a Tris-buffer and oxidation with I$_2$ (Scheme 1B).[52] As a result of our optimization efforts, we found that, by keeping the carbohydrate moiety protected until the last step of the synthesis, we could conduct the first three synthetic steps (SPPS, peptide side chain deprotection, and disulfide bond formation) in one pot without intermittent and inconvenient separations. The different chromatographic properties of the partially and fully unprotected insulin glycoforms (e.g., **23** and **2**, Scheme 1B) made it possible for us to isolate the desired final products from the complex folding mixtures through the combined use of two HPLC purification steps, one before and one after carbohydrate deprotection. The first purification removed the impurities that have different retention times from those of the partially unprotected insulin variants, while the second purification can remove the impurities that have similar chromatographic properties as the variants with unprotected carbohydrates.

Once optimized, our synthetic route allowed us to quickly generate pure and correctly folded insulin glycovariants in milligram scales. Depending on the glycosylation site, the yields ranged from 0.5% to 6.5%. These low yields were likely due to the steric hindrance caused by the side chains of glycoamino acids and the formation of misfolded products.[56] This issue could be addressed by optimizing the reagents and reaction conditions[57] and by recycling the misfolded intermediates.[58] After synthesis, the correct folding, identity, and homogeneity of the synthetic products were confirmed by a combination of circular dichroism (CD, Figure 3), ultraperformance liquid chromatography mass-spectrometry, and Glu-C digestion (Supporting Information).[30,33,52]

The Influence of O-linked GalNAc on the Properties of Human Insulin. With the synthetic insulin glycoforms in hand, we first investigated if O-linked GalNAc at any one of the five glycosylation sites had a particularly strong effect on the stability of human insulin in the presence of proteases. α-Chymotrypsin is a common digestive protease synthesized by the pancreas and secreted into the lumen of the small intestine.[16] This, together with its natural ability to digest insulin, makes it an ideal test of glycosylated insulin's resistance to degradation in the small intestine.[59,60] α-Chymotrypsin cleaves human insulin at the C-terminus of its B chain, an important region for receptor binding and activation, which renders the hormone largely inactive.[60,61] This cleavage also causes an easily detectable change in molecular mass, and therefore each insulin glycoform's half-life toward α-chymotrypsin degradation can be calculated by monitoring the first-order exponential decay of the full-length molecule.[30,60] Quantitative Matrix Assisted Laser Desorption Ionization Time-of-Flight Mass Spectrometry (MALDI-ToF MS) was used to measure the concentration over time.[62] Any change in proteolytic stability introduced by the O-linked glycans on human insulin could then be established by comparing the half-lives of glycoforms **2–6** with that of the unglycosylated insulin **1**.[30,33] As shown in Figure 4A, O-glycosylation with a GalNAcα moiety mostly had a negative impact on the proteolytic stability of human insulin. The unglycosylated insulin **1** has a half-life of α-chymotrypsin degradation of about 10 min, whereas the glycosylated insulin variants **2–4** and **6** have shorter half-lives. Glycoform **5**, which is glycosylated at the ThrB27 site, has a half-life that is comparable to that of the unglycosylated insulin.
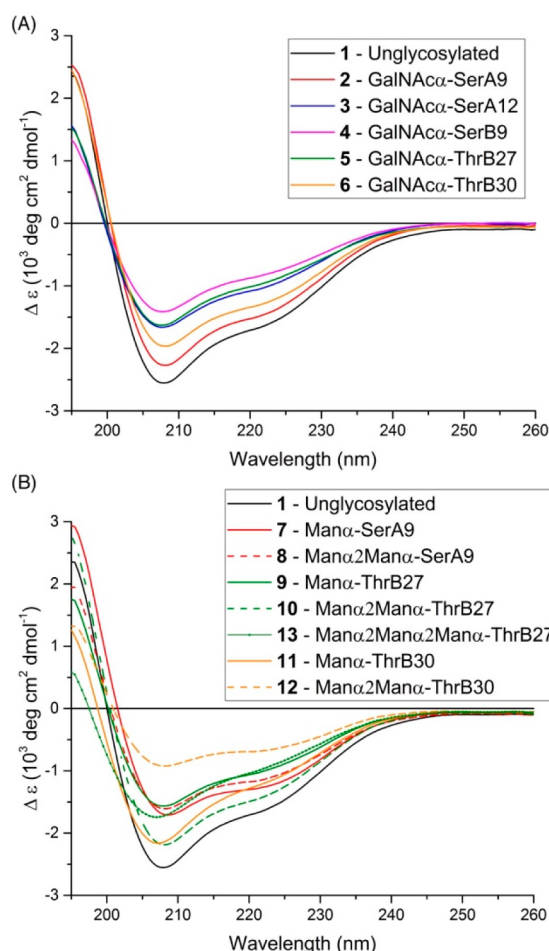
Figure 3. CD spectra collected for unglycosylated insulin[55] and insulin analogs containing GalNAc and Man glycans. Each insulin variant was dissolved in PBS buffer at pH 7.4. Peptide concentration was 0.2 mg mL^{-1} in all tests. CD spectra were obtained at 20 °C with a step of 0.5 nm, 0.5 s per point, and a spectral width of 195−260 nm. All spectra are the average of five scans with an averaged five scan buffer baseline subtracted. The CD spectra of 2−13 are fairly similar to that of 1, indicating that glycosylation does not cause major changes to the secondary structures of the insulin glycovariants.

An ideal insulin product would be tailored for optimal delivery without sacrificing biological activity. In order to test the limits of this idea, we studied the biological activity of insulin through the use of a quantitative fluorescence assay, which relies on detection of the hemagglutinin (HA)-tagged glucose transporter type 4 (GLUT4) on differentiated adipocytes.[63,64] GLUT4 is a glucose transporter that is responsible for insulin-regulated glucose uptake into cells. Insulin can increase the cell-surface level of GLUT4 by stimulating the translocation of GLUT4 to the plasma membrane.[65] Therefore, the biological activity of each insulin glycoform can be quantified by measuring the level of cell-surface GLUT4. The effects of different glycosylation sites, in turn, can be determined by comparing the cell surface GLUT4 levels stimulated by different glycoforms with that of the unglycosylated insulin.[63,64] As shown in Figure 4B, the variants that are glycosylated at the SerA9, ThrB27, and ThrB30 (2, 5, and 6, respectively) had better or similar activities compared to the unglycosylated insulin, while the ones that are glycosylated at the SerA12 and SerB9 sites (3 and 4) exhibited decreased activity. Given that the most stable analog we identified here,
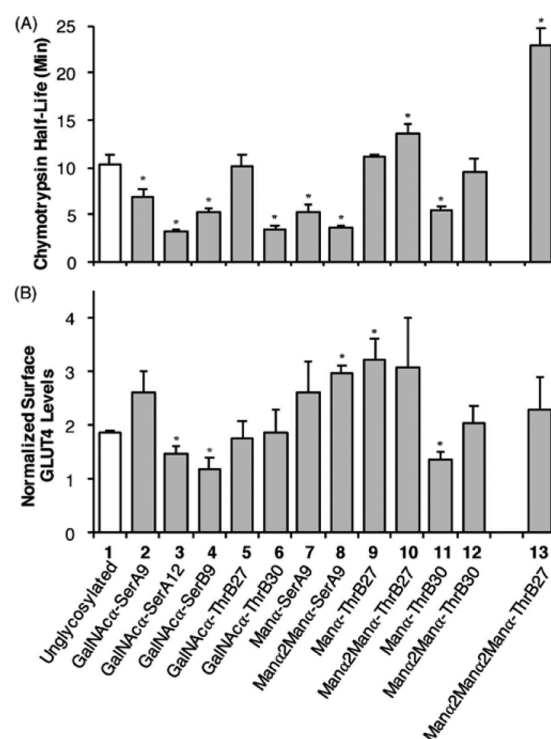

Figure 4. Characterization of synthetic insulin glyco-variants. (A) The effects of O-glycosylation on the proteolytic stability (half-life to α-chymotrypsin degradation). (B) GLUT4 cell surface levels in differentiated adipocytes treated with insulin and its glyco-variants. All error bars reported are standard deviations of data achieved from three separate trials. *Significance at $p < 0.05$.

glycoform 5, was only as good as the unmodified insulin, this pilot study suggests that GalNAc glycans may be not suitable candidates for improving the properties of human insulin.

The Influence of O-Mannosylation on the Properties of Human Insulin. Our previous experience pointed to an alternative type of glycosylation, O-mannosylation, as having the promising ability to improve peptide stability.[33] As demonstrated in our studies of another small protein, a Family 1 carbohydrate-binding module (CBM), O-linked mannose increased both the proteolytic stability and biological activity in a site-specific manner.[30] On the basis of this information, we turned our attention to investigate the effects of O-mannosylation and designed six mono- and dimannosylated insulins: 7−12 (Figure 2). We chose to focus on glycosylation sites SerA9, ThrB27, and ThrB30, which the pilot study had indicated as potentially optimal as compared with other sites.

The insulin glycoforms 7−12 were synthesized, purified, and characterized as described for 2−6 (Supporting Information). As shown in Figure 4A and B, mannosylation of ThrB27 resulted in the best outcome for the 7−12 series, with the mono- and dimannose leading to noticeable increases in both the stability and biological activity. On the basis of previous studies, the increase in stability observed here may be attributed to the additional molecular interactions formed between mannoses and nearby amino acids.[66] The observation that dimannose has a slightly larger effect on the stability prompted us to ask if a trimannose glycan at the same site, which has the potential to introduce more interactions, would result in even further increases. Happily, insulin carrying a trimannose at the ThrB27 site (glycoform 13) displayed a significantly greater

half-life, more than double that of unglycosylated insulin **1**, and a slightly increased biological activity (Figure 4B).

In addition to doubling the proteolytic stability of insulin, we found that *O*-mannosylation could also significantly decrease the oligomerization propensity of insulin.[67] By analyzing the sedimentation velocity through analytical ultracentrifugation, we derived a distribution of insulin molecular species that have different degrees of self-association (Figure 5).[68] The area
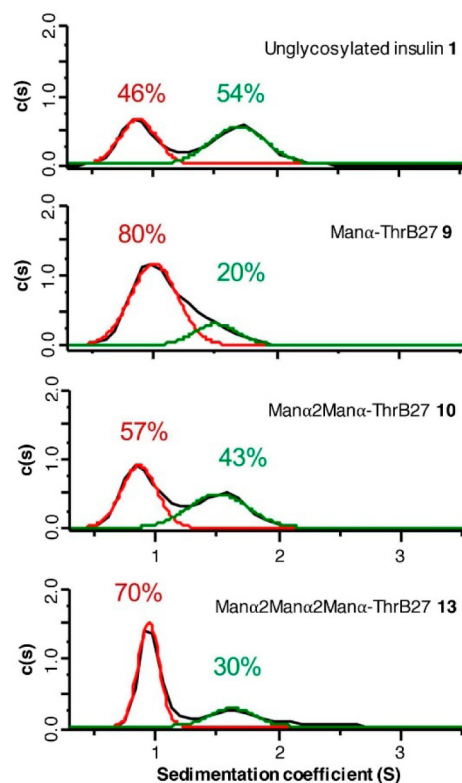

Figure 5. Sedimentation coefficient distributions obtained from sedimentation velocity analysis of insulin variants, with the results for the monomer shown as a red line and for the dimer as a green line.

under each peak gives the relative concentration of that species.[69] As illustrated by the data, trimannosylation at ThrB27 increased the amount of monomer to more than 70% of the sample, whereas amounts of monomer and dimer for unglycosylated **1** were almost equal. Insulin dimers are doubly undesirable in the context of membrane permeability because, not only are they twice as big as monomeric insulin, they are also the first step in formation of hexamers in the presence of Zn^{2+} ions, which will severely limit transit across the intestinal membrane.[70]

CONCLUSIONS

In summary, our work has confirmed that glycoengineering is a feasible approach to increase the stability and decrease the oligomerization of human insulin, both beneficial properties for oral delivery. By systematically comparing the properties of 12 insulin glycoforms with varied glycosylation sites and glycan structures, we have revealed that a specific type of glycan, mannose, is a preferred glycan type, and the unstructured, but functionally critical and degradation/aggregation susceptible, *C*-terminal region of insulin's B-chain is the most productive location for glycan attachment. It is very interesting that we

observed large differences in behavior between mannose- and GalNAc-type glycans at the same location in the peptide sequence. Our recent structural work with the fungal CBM glycopeptide model system has shown that the stereochemical orientation of the hydroxyl group around the carbohydrate ring can lead different glycans to form unique contacts with the peptide.[71] Work by others has also shown that different carbohydrates adopt different orientations with respect to the peptide backbone, which in turn affects the strength of contacts with the peptide portion of the biomolecule.[72] Together, these might help to explain the observed variances that result from glycosylation by different monosaccharides.

Most importantly, we were able to identify one particular glycoform, **13**, with enhanced proteolytic stability, decreased oligomerization propensity, and biological activity comparable to natural insulin. The previous development of a long-acting erythropoiesis stimulating agent, NESP, has demonstrated that even a 2−3 fold increase in stability can translate to large changes *in vivo* for protein and peptide therapeutics.[73] Thus, the doubling of insulin's degradation half-life should lead to significant improvements *in vivo*. Additionally, because different glycan structures can have unique effects on insulin's properties and glycans at different sites may synergistically alter some of those properties,[30] it is reasonable to believe that further movement toward oral delivery could be achieved by wider exploration of glycan structures at ThrB27. Potential advances might also be found in synergistic effects that could result from the glycosylation of nearby ThrB30. Studies of the effects of glycosylation on the *in vivo* behavior and immunogenicity of insulin analogs in animal models and the search for further improvements in properties for oral delivery are currently being pursued, and results will be reported soon.

METHODS

Materials and Methods. All commercial reagents and solvents were used as received. Unless otherwise noted, all reactions and purifications were performed under air atmosphere at RT. All LC-MS analyses were performed using a Waters Acquity Ultra Performance LC system equipped with an Acquity UPLC BEH 300 C4, 1.7 μm, 2.1 × 100 mm column at flow rates of 0.3 and 0.5 mL/min. The mobile phase for LC-MS analysis was a mixture of H_2O (0.1% formic acid, v/v) and acetonitrile (0.1% formic acid, v/v). All preparative separations were performed using a LabAlliance HPLC solvent delivery system equipped with a Rainin UV-1 detector and a Varian Microsorb 100−5, C18 250 × 21.4 mm column at a flow rate of 16.0 mL/min. The mobile phase for HPLC purification was a mixture of H_2O (0.05% TFA, v/v) and acetonitrile (0.04% TFA, v/v). A Waters SYNAPT G2 Qtof system was used for mass spectrometric analysis.

Synthesis of Glycoamino Acids. The glycoamino acid building blocks Fmoc-Ser(Ac₃GalNAcα)-OH, Fmoc-Thr(Ac₃GalNAcα)-OH, Fmoc-Ser(Ac₄Manα)-OH, Fmoc-Ser(Ac₄Manα2Ac₃Manα)-OH, Fmoc-Thr(Ac₄Manα)-OH, Fmoc-Thr(Ac₄Manα2Ac₃Manα)-OH, and Fmoc-Thr(Ac₄Manα2Ac₃Manα2Ac₃Manα)-OH were prepared following previous procedures.[30,33] H-Thr(Ac₃GalNAcα)-O*t*-Bu, H-Thr-(Ac₄Manα)-O*t*-Bu, and H-Thr(Ac₄Manα2Ac₃Manα)-O*t*-Bu were prepared using procedures adapted from previous work.[30,33]

Solid-Phase Peptide Synthesis, Cleavage, and Activation. Automated peptide synthesis was performed on an Applied Biosystems Pioneer continuous flow peptide synthesizer. Peptides were synthesized under standard automated Fmoc conditions. The deblock solution was a mixture of 100/5/5 of DMF/piperidine/DBU. Fmoc protected amino acid (4.0 equiv), HATU (4.0 equiv), and DIEA (8.0 equiv) were used for the coupling steps.

Synthesis of A-Chain. The synthesis of the unglycosylated A chain [IVEQC(Acm)CTSIC(Acm)SLYQLENYC(Acm)N] was based on the previous route.[52] The synthesis was conducted on 0.05 mmol

Fmoc-Asn-NovaSyn TGT resin from EMD Millipore. After cleavage from the resin by 10 mL of TFA/TIS/H$_2$O (95:2.5:2.5) and being precipitated by cold ether, the crude peptide was dissolved in 20 mL of MeCN/H$_2$O (1:1) and lyophilized to dryness for the next synthesis step without further purification.

Synthesis of Glycosylated A-Chains. The synthesis of each glycosylated A chain [GIVEQC(Acm)CTSIC(Acm)SLYQLENYC-(Acm)N, underlined amino acids are designed glycosylation sites] was conducted similar to the unglycosylated A-chain except that Fmoc-Ser(Ac$_3$GalNAcα)-OH, Fmoc-Ser(Ac$_4$Manα)-OH, or Fmoc-Ser(Ac$_4$Manα2Ac$_3$Manα1)-OH was used to introduce desired sugars to the peptides as building blocks.

Synthesis of B-Chain. The synthesis of the unglycosylated B chain [FVNQHLC(SPy)GSHLVEALYLVC(Acm)GERGFFYTPKT] was based on the previous route.[52] The synthesis of the B chain was conducted on 0.05 mmol Fmoc-Thr-NovaSyn TGT resin from EMD Millipore. Cleavage was conducted by treating the 0.05 mmol resin with 10 mL of TFA/TIS/H$_2$O (95:2.5:2.5) that also contained 20.0 equiv of 2,2′-dithiodipyridine (DTDP, 0.22 g) at RT for 2 h. The resin was filtered. The solvent was evaporated under a stream of condensed air, and then the remaining residue was precipitated in cold ether (30 mL). The precipitate was collected by centrifugation and then washed with cold ether (30 mL × 3). The crude peptide was dissolved in 20 mL of MeCN/H$_2$O (1:1) and lyophilized to dryness. Crude peptide was used in the next synthesis step without further purification.

Synthesis of Glycosylated B-Chains. The synthesis of each B chain that is glycosylated either at Ser9 or at Thr27 [FVNQHLC-(SPy)GSHLVEALYLVC(Acm)GERGFFYTPKT, underlined amino acids are designed glycosylation sites] was conducted similar to the unglycosylated B chain except that Fmoc-Ser(Ac$_3$GalNAcα)-OH, Fmoc-Thr(Ac$_3$GalNAcα)-OH, Fmoc-Thr(Ac$_4$Manα)-OH, Fmoc-Thr-(Ac$_4$Manα2Ac$_3$Manα)-OH, or Fmoc-Thr-(Ac$_4$Manα2Ac$_3$Manα2Ac$_3$Manα)-OH was used to introduce the desired sugars to the peptides as building blocks.

For the synthesis of each B chain that is glycosylated at Thr30, [FVNQHLC(SPy)GSHLVEALYLVC(Acm)GERGFFYTPKT, underlined amino acids are designed glycosylation sites], the fully protected peptide Boc-FVNQHLC(Trt)GSHLVEALYLVC(Acm)-GERGFFYTPK-OH was synthesized on 0.05 mmol Fmoc-Lys-NovaSyn TGT resin from EMD Millipore. Cleavage was conducted by treating the 0.05 mmol resin with 10 mL of DCM/TFE/AcOH (8:1:1) at RT for 2 h. After cleavage, lyophilized crude peptide was collected from the resin suspension using the same procedures as the unglycosylated B -chain. The fully protected peptide (0.0185 mmol, 1.1 equiv) and glycosylated Thr building blocks (0.0168 mmol, 1.0 equiv); H-Thr(Ac$_3$GalNAcα1)-Ot-Bu, H-Thr(Ac$_4$Manα)-Ot-Bu or H-Thr(Ac$_4$Manα2Ac$_3$Manα)-Ot-Bu were dissolved in 710 μL of CHCl$_3$/TFE (3:1). The mixture was cooled to −10 °C, and then HOOBt (0.0185 mmol, 1.1 equiv) and EDCI (0.0185 mmol, 1.1 equiv) were added. The mixture was stirred at RT for 3 h with a centrifuge every 30 min. After 3 h, the solvent was blown away by condensed air, and 1 mL of AcOH/H$_2$O (1:20) was added. The supernatant was discarded after centrifugation, and the residue was dissolved in 4 mL of TFA/TIS/H$_2$O (95:2.5:2.5) that also contained 20.0 equiv of DTDP (0.088 g) at RT for 2 h. The resin was filtered. The solvent was evaporated under a stream of condensed air, and then the remaining residue was precipitated in cold ether (15 mL). The precipitate was collected by centrifugation and then washed with cold ether (15 mL × 3). The crude peptide was dissolved in 10 mL of MeCN/H$_2$O (1:1) and lyophilized to dryness. Lyophilized crude peptide was used in the next synthesis step without further purification.

Unglycosylated Insulin Folding and Purification. The folding of unglycosylated insulin was based on the previous route.[52] A chain (0.02 mmol, 1.0 equiv) and B chain (0.0204 mmol, 1.2 equiv) were mixed in 2 mL of 8 M Gn·HCl and 0.1 M Tris buffer (pH 8.8). The mixture was vortexed vigorously until fully dissolved, and then the pH was raised to 8 by adding 20 μL of 2 M NaOH (monitored by pH strip). This solution was stirred for 5 min before being diluted by 16 mL of AcOH/H$_2$O (4:1), followed by treatment with I$_2$ (0.282 g) in MeOH (3.2 mL) for 15 min at RT. Then, this mixture was treated

with 1.0 M aqueous ascorbic acid (4.8 mL), diluted with H$_2$O (20 mL), and loaded onto preparative RP-HPLC for purification. The products were detected by UV absorption at 230 nm. After HPLC purification with a linear gradient of 20 → 50% MeCN in H$_2$O over 30 min, the fractions were collected and checked by LC-MS. The pure fractions with the desired mass and shortest retention time were combined and lyophilized to give the desired product as a white powder.

Glycosylated Insulin Folding and Purification. A-chain and B-chain peptides carrying the desired glycosylation patterns were combined and folded exactly as for unglycosylated insulin. HPLC purification was done exactly as with unglycosylated insulin except a linear gradient of 25 → 60% MeCN in H$_2$O over 30 min was used. After HPLC purification the Ac-protected product was lyophilized to dryness and used in the final Ac removal step.

Glycosylated Insulin Ac Removal. The lyophilized Ac-protected product was dissolved in 1 mL of hydrazine/H$_2$O (1:20) and stirred at RT for 30 min. Then, the reaction was quenched with 1 mL of AcOH/H$_2$O (1:20). HPLC purification was done exactly as with glycosylated insulin before Ac removal.

Glu-C Digestion. Glycosylated insulins (100 μg) were mixed with 10 μg of Glu-C in 100 μL of 50 mM Tris buffer (pH 8.0) at RT and allowed to stand for 2 h before being analyzed by LC-MS.[52]

Chymotrypsin Digestion of Glycosylated Synthetic Insulin Glycoforms 2−13.[60] A total of 76 μL of a 0.5 μg/μL insulin solution was prepared in a buffer composed of 100 mM Tris and 1 mM CaCl$_2$ adjusted to pH 8.0. Prior to digestion, this insulin solution was equilibrated to 37 °C for 15 min. Immediately before the addition of digestion enzyme, the insulin solution was vortexed for 2 s, and a 1 μL of sample was taken as the zero-time sample and immediately added to 9.0 μL of a 0.2% TFA solution containing 0.055 μg/μL of unglycosylated synthetic insulin 1 as an internal standard. Digestion was begun by adding 4 μL of an α-chymotrypsin stock solution (0.25 μg/μL enzyme in a buffer composed of 100 mM Tris and 1 mM CaCl$_2$ adjusted to pH 8.0) to reach a final enzyme concentration of 0.0125 μg/μL. The resulting solution was vortexed for 2 s and incubated at 37 °C. After 1, 3, 5, 10, 20, 30, 40, 60, 90, 120, and 180 min, 1 μL aliquots were removed from the digestion reaction and added to 9.0 μL of a 0.2% TFA solution containing 0.055 μg/μL unglycosylated synthetic insulin 1 as an internal standard. These samples were vortexed for 2 s and stored at −20 °C until MALDI-TOF MS analysis could be carried out. MALDI-TOF analysis was done according to previous procedures.[30]

Chymotrypsin Digestion of Unglycosylated Synthetic Insulin Glycoform 1. Digestion and analysis of 1 was done exactly as described above for 2−13 except glycosylated synthetic insulin 5 was used as the internal standard during quantitative MALDI-TOF MS analysis.

Cell Culture and Differentiation. Mouse preadipocytes (derived from inguinal white adipocyte tissues, gift from Dr. Shingo Kajimura) were maintained in Dulbecco's Modified Eagle Medium (DMEM) supplemented with 10% FBS and penicillin/streptomycin. To differentiate into adipocytes, preadipocytes were cultured to ~95% confluence before a differentiation cocktail was added to the following concentrations: 5 μg/mL of insulin (Sigma, #I0516), 1 nM T3 (Sigma, #T2877), 125 mM indomethacin (Sigma, #I-7378), 5 μM dexamethasone (Sigma, #D1756), and 0.5 mM IBMX (Sigma, #I5879). After 2 days, the cells were switched to DMEM supplemented with 10% FBS, 5 μg/mL of insulin, and 1 nM T3. After another 2 days, fresh media of the same composition were supplied. Differentiated adipocytes were usually analyzed 6 days after the addition of the differentiation cocktail.

To generate cell lines expressing the GFP-GLUT4-HA reporter, lentiviruses were produced by transfecting 293T cells with a mixture of plasmids including GFP-GLUT4-HA,[74] pAdVAntage (Promega, #E1711), pCMV-VSVG, and psPax2. Lentiviral particles were collected 40 h after transfection and every 24 h thereafter for a total of four collections. Lentiviruses were pooled and concentrated by centrifugation in a Beckman SW28 rotor at 25 000 rpm for 1.5 h. The viral pellets were resuspended in PBS and were used to transduce preadipocytes.

Flow Cytometry Analysis of Insulin-Triggered Glut4 Translocation. Differentiated adipocytes were washed three times with the KRH buffer (121 mM NaCl, 4.9 mM KCl, 1.2 mM MgSO$_4$, 0.33 mM CaCl$_2$, and 12 mM HEPES, pH 7.0). After incubation in the KRH buffer for 2 h, the cells were treated with 100 nM insulin for 30 min. When applicable, 100 nM wortmannin (Sigma, #W1628) was added 10 min prior to insulin treatment. After insulin stimulation, the cells were rapidly chilled on an ice bath, and their surface reporters were stained using anti-HA antibodies (BioLegend, #901501) and allophycocyanin (APC)-conjugated secondary antibodies (eBioscience, #17−4014). The cells were dissociated from the plates using Accutase (Innovative Cell Technologies, #AT 104), and their APC and GFP fluorescence was measured on a CyAN ADP analyzer. Data were analyzed using the FlowJo software.

Analytical Ultracentrifugation (AUC) Analysis. Analytical ultracentrifugation (AUC) experiments were carried out on a Beckman Coulter ProteomeLab XL-I protein characterization system equipped with a four-hole An60 Ti rotor. Data were collected using the ProteomeLab XL-I absorbance optical system at a wavelength of 240 nm. A total of 200 μg of each insulin variant was dissolved in 500 μL of PBS buffer (pH 7.4) to give a final concentration of 0.4 mg mL^{-1}. These samples were loaded into 12 mm standard double-sector aluminum and charcoal-filled Epon centerpieces with sapphire windows. PBS buffer alone was used as an optical reference. Experiments were run at 20 °C and 60 krpm. Raw AUC data were analyzed with the SEDFIT program, then fit using Origin's Nonlinear Gauss Curve Fit application. Each curve was centered on a fixed value with other parameters allowed to float. This gave approximations of Gauss-shaped distribution curves for each individual species in each AUC run, and the area under each of these fit curves was used to approximate the abundance of each molecular species in each sample.

■ ASSOCIATED CONTENT

Ⓢ Supporting Information

The Supporting Information is available free of charge on the ACS Publications website at DOI: 10.1021/acschembio.7b00794.

> LC traces and MS spectra for each insulin glycovariant 1−13; LC traces, MS spectra, and cleavage maps for confirmation of disulfide bond patterns in glycosylated insulins 2, 4, and 5; proteolytic degradation half-life values of glycosylated insulins 1−13; fluorescence ratio values from GLUT4 translocation assay for glycosylated insulins 1−13 (PDF)

■ AUTHOR INFORMATION

Corresponding Authors
*E-mail: weixx@sun5.ibp.ac.cn.
*E-mail: jingshi.shen@colorado.edu.
*E-mail: zhongping.tan@colorado.edu.

ORCID Ⓘ
Xinfeng Wang: 0000-0002-6399-1011
Zhongping Tan: 0000-0002-9302-150X

Author Contributions
‖These authors contributed equally. All authors have given approval to the final version of the manuscript.

Notes
The authors declare no competing financial interest.

■ ACKNOWLEDGMENTS

■ REFERENCES

(1) *Global report on diabetes*. Geneva: World Health Organization, 2016.

(2) White, J. R., Jr. (2014) A brief history of the development of diabetes medications. *Diabetes Spectr. 27*, 82−86.

(3) Brown, T. L., and Meloche, T. M. (2016) Exome sequencing a review of new strategies for rare genomic disease research. *Genomics 108*, 109−114.

(4) Hanefeld, M. (2014) Use of insulin in type 2 diabetes: what we learned from recent clinical trials on the benefits of early insulin initiation. *Diabetes Metab. 40*, 391−399.

(5) Davies, M. (2004) The reality of glycaemic control in insulin treated diabetes: defining the clinical challenges. *Int. J. Obes. 28* (Suppl 2), S14−S22.

(6) Tibaldi, J. M. (2012) Evolution of insulin development: focus on key parameters. *Adv. Ther. 29*, 590−619.

(7) Garcia-Perez, L. E., Alvarez, M., Dilla, T., Gil-Guillen, V., and Orozco-Beltran, D. (2013) Adherence to therapies in patients with type 2 diabetes. *Diabetes Ther. 4*, 175−194.

(8) Pandyarajan, V., and Weiss, M. A. (2012) Design of non-standard insulin analogs for the treatment of diabetes mellitus. *Curr. Diabetes Rep. 12*, 697−704.

(9) Verma, A., Kumar, N., Malviya, R., and Sharma, P. K. (2014) Emerging trends in noninvasive insulin delivery. *J. Pharm. 2014*, 1−9.

(10) Iyer, H., Khedkar, A., and Verma, M. (2010) Oral insulin - a review of current status. *Diabetes, Obes. Metab. 12*, 179−185.

(11) Arbit, E., and Kidron, M. (2009) Oral insulin: the rationale for this approach and current developments. *J. Diabetes Sci. Technol. 3*, 562−567.

(12) Zaykov, A. N., Mayer, J. P., and DiMarchi, R. D. (2016) Pursuit of a perfect insulin. *Nat. Rev. Drug Discovery 15*, 425−439.

(13) Muheem, A., Shakeel, F., Jahangir, M. A., Anwar, M., Mallick, N., Jain, G. K., Warsi, M. H., and Ahmad, F. J. (2016) A review on the strategies for oral delivery of proteins and peptides and their clinical perspectives. *Saudi Pharm. J. 24*, 413−428.

(14) Fonte, P., Araujo, F., Reis, S., and Sarmento, B. (2013) Oral insulin delivery: how far are we? *J. Diabetes Sci. Technol. 7*, 520−531.

(15) Kalra, S., Kalra, B., and Agrawal, N. (2010) Oral insulin. *Diabetol. Metab. Syndr. 2*, 66.

(16) Elsayed, A. M. (2012) *Oral delivery of insulin: novel approaches*, pp 282−314, INTECH Open Access Publisher.

(17) Yin, N., Brimble, M. A., Harris, P. W., and Wen, J. (2014) Enhancing the oral bioavailability of peptide drugs by using chemical modification and other Approaches. *Med. Chem. 4*, 763−769.

(18) Fujii, S., Yokoyama, T., Ikegaya, K., Sato, F., and Yokoo, N. (1985) Promoting effect of the new chymotrypsin inhibitor FK-448 on the intestinal absorption of insulin in rats and dogs. *J. Pharm. Pharmacol. 37*, 545−549.

(19) Di, L. (2015) Strategic approaches to optimizing peptide ADME properties. *AAPS J. 17*, 134−143.

(20) Varki, A. (2009) *Essentials of glycobiology*; Cold Spring Harbor Laboratory Press: Cold Spring Harbor, N.Y..

(21) Chen, M. M., Bartlett, A. I., Nerenberg, P. S., Friel, C. T., Hackenberger, C. P., Stultz, C. M., Radford, S. E., and Imperiali, B. (2010) Perturbing the folding energy landscape of the bacterial immunity protein Im7 by site-specific N-linked glycosylation. *Proc. Natl. Acad. Sci. U. S. A. 107*, 22528−22533.

(22) Uchio, T., Baudys, M., Liu, F., Song, S. C., and Kim, S. W. (1999) Site-specific insulin conjugates with enhanced stability and extended action profile. *Adv. Drug Delivery Rev. 35*, 289−306.

(23) Gribben, J. G., Devereux, S., Thomas, N. S., Keim, M., Jones, H. M., Goldstone, A. H., and Linch, D. C. (1990) Development of antibodies to unprotected glycosylation sites on recombinant human GM-CSF. *Lancet 335*, 434−437.

(24) Ragnhammar, P., Friesen, H. J., Frodin, J. E., Lefvert, A. K., Hassan, M., Osterborg, A., and Mellstedt, H. (1994) Induction of anti-recombinant human granulocyte-macrophage colony-stimulating factor (Escherichia coli-derived) antibodies and clinical effects in nonimmunocompromised patients. *Blood* 84, 4078−4087.

(25) Hinds, K. D., and Kim, S. W. (2002) Effects of PEG conjugation on insulin properties. *Adv. Drug Delivery Rev.* 54, 505−530.

(26) Calceti, P., Salmaso, S., Walker, G., and Bernkop-Schnurch, A. (2004) Development and in vivo evaluation of an oral insulin-PEG delivery system. *Eur. J. Pharm. Sci.* 22, 315−323.

(27) Shental-Bechor, D., and Levy, Y. (2008) Effect of glycosylation on protein folding: a close look at thermodynamic stabilization. *Proc. Natl. Acad. Sci. U. S. A.* 105, 8256−8261.

(28) Elliott, S. (2009) Glycoengineering of erythropoietin, in *post-translational modification of protein biopharmaceuticals*, Wiley-VCH Verlag GmbH & Co. KGaA, 295−317.

(29) Price, J. L., Shental-Bechor, D., Dhar, A., Turner, M. J., Powers, E. T., Gruebele, M., Levy, Y., and Kelly, J. W. (2010) Context-dependent effects of asparagine glycosylation on Pin WW folding kinetics and thermodynamics. *J. Am. Chem. Soc.* 132, 15359−15367.

(30) Chen, L., Drake, M. R., Resch, M. G., Greene, E. R., Himmel, M. E., Chaffey, P. K., Beckham, G. T., and Tan, Z. (2014) Specificity of O-glycosylation in enhancing the stability and cellulose binding affinity of Family 1 carbohydrate-binding modules. *Proc. Natl. Acad. Sci. U. S. A.* 111, 7612−7617.

(31) Price, J. L., Culyba, E. K., Chen, W., Murray, A. N., Hanson, S. R., Wong, C. H., Powers, E. T., and Kelly, J. W. (2012) N-glycosylation of enhanced aromatic sequons to increase glycoprotein stability. *Biopolymers* 98, 195−211.

(32) Hanson, S. R., Culyba, E. K., Hsu, T. L., Wong, C. H., Kelly, J. W., and Powers, E. T. (2009) The core trisaccharide of an N-linked glycoprotein intrinsically accelerates folding and enhances stability. *Proc. Natl. Acad. Sci. U. S. A.* 106, 3131−3136.

(33) Guan, X., Chaffey, P. K., Zeng, C., Greene, E. R., Chen, L., Drake, M. R., Chen, C., Groobman, A., Resch, M. G., Himmel, M. E., Beckham, G. T., and Tan, Z. (2015) Molecular-scale features that govern the effects of O-glycosylation on a carbohydrate-binding module. *Chem. Sci.* 6, 7185−7189.

(34) Ladisch, M. R., and Kohlmann, K. L. (1992) Recombinant human insulin. *Biotechnol. Prog.* 8, 469−478.

(35) Baeshen, N. A., Baeshen, M. N., Sheikh, A., Bora, R. S., Ahmed, M. M., Ramadan, H. A., Saini, K. S., and Redwan, E. M. (2014) Cell factories for insulin production. *Microb. Cell Fact.* 13, 141.

(36) Belgi, A., Hossain, M. A., Tregear, G. W., and Wade, J. D. (2011) The chemical synthesis of insulin: from the past to the present. *Immunol., Endocr. Metab. Agents Med. Chem.* 11, 40−47.

(37) Liu, F., Zaykov, A. N., Levy, J. J., DiMarchi, R. D., and Mayer, J. P. (2016) Chemical synthesis of peptides within the insulin superfamily. *J. Pept. Sci.* 22, 260−270.

(38) Avital-Shmilovici, M., Mandal, K., Gates, Z. P., Phillips, N. B., Weiss, M. A., and Kent, S. B. (2013) Fully convergent chemical synthesis of ester insulin: determination of the high resolution X-ray structure by racemic protein crystallography. *J. Am. Chem. Soc.* 135, 3173−3185.

(39) Sohma, Y., Hua, Q. X., Whittaker, J., Weiss, M. A., and Kent, S. B. (2010) Design and folding of [GluA4(ObetaThrB30)]insulin ("ester insulin"): a minimal proinsulin surrogate that can be chemically converted into human insulin. *Angew. Chem., Int. Ed.* 49, 5489−5493.

(40) Bertozzi, C. R., and Kiessling, L. L. (2001) Chemical glycobiology. *Science* 291, 2357−2364.

(41) Buskas, T., Ingale, S., and Boons, G. J. (2006) Glycopeptides as versatile tools for glycobiology. *Glycobiology* 16, 113R−136R.

(42) Gamblin, D. P., Scanlan, E. M., and Davis, B. G. (2009) Glycoprotein synthesis: an update. *Chem. Rev.* 109, 131−163.

(43) Tsai, Y. H., Liu, X., and Seeberger, P. H. (2012) Chemical biology of glycosylphosphatidylinositol anchors. *Angew. Chem., Int. Ed.* 51, 11438−11456.

(44) Dulaney, S. B., and Huang, X. (2012) Strategies in synthesis of heparin/heparan sulfate oligosaccharides: 2000-present. *Adv. Carbohydr. Chem. Biochem.* 67, 95−136.

(45) Horiya, S., MacPherson, I. S., and Krauss, I. J. (2014) Recent strategies targeting HIV glycans in vaccine design. *Nat. Chem. Biol.* 10, 990−999.

(46) Fernandez-Tejada, A., Brailsford, J., Zhang, Q., Shieh, J. H., Moore, M. A., and Danishefsky, S. J. (2014) Total synthesis of glycosylated proteins. *Top. Curr. Chem.* 362, 1−26.

(47) Krasnova, L., and Wong, C. H. (2016) Understanding the chemistry and biology of glycosylation with glycan synthesis. *Annu. Rev. Biochem.* 85, 599−630.

(48) Pan, M., Li, S., Li, X., Shao, F., Liu, L., and Hu, H.-G. (2014) Synthesis of and specific antibody generation for glycopeptides with arginine N-glcNAcylation. *Angew. Chem., Int. Ed.* 53, 14517−14521.

(49) Chen, W., Enck, S., Price, J. L., Powers, D. L., Powers, E. T., Wong, C. H., Dyson, H. J., and Kelly, J. W. (2013) Structural and energetic basis of carbohydrate-aromatic packing interactions in proteins. *J. Am. Chem. Soc.* 135, 9877−9884.

(50) Wang, P., Dong, S., Shieh, J. H., Peguero, E., Hendrickson, R., Moore, M. A., and Danishefsky, S. J. (2013) Erythropoietin derived by chemical synthesis. *Science* 342, 1357−1360.

(51) Hsieh, Y. S., Wijeyewickrema, L. C., Wilkinson, B. L., Pike, R. N., and Payne, R. J. (2014) Total synthesis of homogeneous variants of hirudin P6: a post-translationally modified anti-thrombotic leech-derived protein. *Angew. Chem., Int. Ed.* 53, 3947−3951.

(52) Liu, F., Luo, E. Y., Flora, D. B., and Mayer, J. P. (2013) Concise synthetic routes to human insulin. *Org. Lett.* 15, 960−963.

(53) Tan, Z., Shang, S., Halkina, T., Yuan, Y., and Danishefsky, S. J. (2009) Toward homogeneous erythropoietin: non-NCL-based chemical synthesis of the Gln78-Arg166 glycopeptide domain. *J. Am. Chem. Soc.* 131, 5424−5431.

(54) Tan, Z., Shang, S., and Danishefsky, S. J. (2010) Insights into the finer issues of native chemical ligation: an approach to cascade ligations. *Angew. Chem., Int. Ed.* 49, 9500−9503.

(55) Lopes, M. A., Abrahim-Vieira, B., Oliveira, C., Fonte, P., Souza, A. M., Lira, T., Sequeira, J. A., Rodrigues, C. R., Cabral, L. M., Sarmento, B., Seica, R., Veiga, F., and Ribeiro, A. J. (2015) Probing insulin bioactivity in oral nanoparticles produced by ultrasonication-assisted emulsification/internal gelation. *Int. J. Nanomed.* 10, 5865−5880.

(56) Murakami, M., Kiuchi, T., Nishihara, M., Tezuka, K., Okamoto, R., Izumi, M., and Kajihara, Y. (2016) Chemical synthesis of erythropoietin glycoforms for insights into the relationship between glycosylation pattern and bioactivity. *Sci. Adv.* 2, e1500678.

(57) Bray, B. L. (2003) Large-scale manufacture of peptide therapeutics by chemical synthesis. *Nat. Rev. Drug Discovery* 2, 587−593.

(58) Gould, A., Ji, Y., Aboye, T. L., and Camarero, J. A. (2011) Cyclotides, a novel ultrastable polypeptide scaffold for drug discovery. *Curr. Pharm. Des.* 17, 4294−4307.

(59) Liu, F. Y., Kildsig, D. O., and Mitra, A. K. (1991) Insulin aggregation in aqueous media and its effect on alpha-chymotrypsin-mediated proteolytic degradation. *Pharm. Res.* 8, 925−929.

(60) Schilling, R. J., and Mitra, A. K. (1991) Degradation of insulin by trypsin and alpha-chymotrypsin. *Pharm. Res.* 8, 721−727.

(61) Ciszak, E., Beals, J. M., Frank, B. H., Baker, J. C., Carter, N. D., and Smith, G. D. (1995) Role of C-terminal B-chain residues in insulin assembly: the structure of hexameric LysB28ProB29-human insulin. *Structure* 3, 615−622.

(62) Duncan, M. W., Roder, H., and Hunsucker, S. W. (2008) Quantitative matrix-assisted laser desorption/ionization mass spectrometry. *Briefings Funct. Genomics Proteomics* 7, 355−370.

(63) Zeigerer, A., Lampson, M. A., Karylowski, O., Sabatini, D. D., Adesnik, M., Ren, M., and McGraw, T. E. (2002) GLUT4 retention in adipocytes requires two intracellular insulin-regulated transport steps. *Mol. Biol. Cell* 13, 2421−2435.

(64) van Dam, E. M., Govers, R., and James, D. E. (2005) Akt activation is required at a late stage of insulin-induced GLUT4

translocation to the plasma membrane. *Mol. Endocrinol. 19*, 1067–1077.

(65) Muretta, J. M., and Mastick, C. C. (2009) How insulin regulates glucose transport in adipocytes. *Vitam. Horm. 80*, 245–286.

(66) Sola, R. J., and Griebenow, K. (2009) Effects of glycosylation on the stability of protein pharmaceuticals. *J. Pharm. Sci. 98*, 1223–1245.

(67) Nettleton, E. J., Tito, P., Sunde, M., Bouchard, M., Dobson, C. M., and Robinson, C. V. (2000) Characterization of the oligomeric states of insulin in self-assembly and amyloid fibril formation by mass spectrometry. *Biophys. J. 79*, 1053–1065.

(68) Berkowitz, S. A. (2006) Role of analytical ultracentrifugation in assessing the aggregation of protein biopharmaceuticals. *AAPS J. 8*, E590–605.

(69) Cole, J. L., Lary, J. W., Moody, T. P., and Laue, T. M. Analytical ultracentrifugation: sedimentation velocity and sedimentation equilibrium. *Biophysical Tools for Biologists, Volume One: In Vitro Techniques*, Methods in Cell Biology; Elsevier, 2008, vol *84*, pp 143–179, DOI: 10.1016/S0091-679X(07)84006-4.

(70) Dodson, E. J., Dodson, G. G., Hubbard, R. E., Moody, P. C. E., Turkenburg, J., Whittingham, J., Xiao, B., Brange, J., Kaarsholm, N., and Thogersen, H. (1993) Insulin assembly: its modification by protein engineering and ligand binding. *Philos. Trans. R. Soc., A 345*, 153–164.

(71) Chaffey, P. K., Guan, X., Chen, C., Ruan, Y., Wang, X., Tran, A. H., Koelsch, T. N., Cui, Q., Feng, Y., and Tan, Z. (2017) Structural insight into the stabilizing effect of O-glycosylation. *Biochemistry 56*, 2897–2906.

(72) Hsu, C. H., Park, S., Mortenson, D. E., Foley, B. L., Wang, X., Woods, R. J., Case, D. A., Powers, E. T., Wong, C. H., Dyson, H. J., and Kelly, J. W. (2016) The Dependence of carbohydrate-aromatic interaction strengths on the structure of the carbohydrate. *J. Am. Chem. Soc. 138*, 7636–7648.

(73) Sinclair, A. M., and Elliott, S. (2005) Glycoengineering: the effect of glycosylation on the properties of therapeutic proteins. *J. Pharm. Sci. 94*, 1626–1635.

(74) Muretta, J. M., Romenskaia, I., and Mastick, C. C. (2008) Insulin releases Glut4 from static storage compartments into cycling endosomes and increases the rate constant for Glut4 exocytosis. *J. Biol. Chem. 283*, 311–323.